

From classical to quantum walks with stochastic resetting on networks

Sascha Wald^{1,*} and Lucas Böttcher^{2,3,4,†}

¹*Max-Planck-Institut für Physik Komplexer Systeme, Nöthnitzer Straße 38, D-01187, Dresden, Germany*

²*Computational Medicine, UCLA, 90024, Los Angeles, United States*

³*Institute for Theoretical Physics, ETH Zurich, 8093, Zurich, Switzerland*

⁴*Center of Economic Research, ETH Zurich, 8092, Zurich, Switzerland*

(Dated: May 31, 2022)

Random walks are fundamental models of stochastic processes with applications in various fields including physics, biology, and computer science. We study classical and quantum random walks under the influence of stochastic resetting on arbitrary networks. Based on the mathematical formalism of quantum stochastic walks, we provide a unifying description of classical and quantum walks whose evolution is determined by graph Laplacians. We study the influence of quantum effects on the stationary and long-time average probability distribution by interpolating between the classical and quantum regime. We compare our analytical results on stationary and long-time average probability distributions with numerical simulations on different networks, revealing significant differences in the way resets affect the sampling properties of classical and quantum walks.

I. INTRODUCTION

Karl Pearson coined the term “random walk” in a short commentary article in 1905 [1]. In the same year Albert Einstein described the random movements of particles suspended in a fluid in terms of Brownian motion [2, 3], illustrating the potential of stochastic descriptions to improve our understanding of physical processes.

Early versions of random walks were also applied to problems in probability theory (see, e.g., the “gambler’s ruin” problem [4]) or in materials science (e.g., for describing particle-level dynamics in the formation of polymer chains [5–7]). Nowadays, the area of applications of random walks is quite versatile: adapted formulations of random walks are common tools in quantitative finance to mathematically describe stock-price fluctuations [8, 9], but random walks are also applied in the study of foraging animals [10, 11] and in the context of efficient search algorithms [12] such as the famous PageRank [13]. Even as models of opinion formation, random walks were able to provide insights into the mechanisms of consensus and opinion polarization [14–16]. We could continue this list with many more examples from various disciplines, but instead refer the interested reader to Refs. [17–19] for more information on different formulations of random walks and their study on different network structures.

Extensions of classical random walks (CRWs) to the quantum realm [22] led to the development of hybrid classical-quantum versions of the PageRank [23], new classes of quantum algorithms [24–27], and important insights into the feasibility of quantum computations in terms of quantum walks (QWs) [28]. In fact, any quantum computation can be performed by a QW on an unweighted low-degree graph (i.e., a network with a sparse

binary adjacency matrix) [28]. In this work, we shall focus on walks that are induced by graph Laplacians. Note that different formulations of QWs have been proposed, including coined QWs [29, 30] based on “coin flip” and position shift operators acting on spin and position states, or the formalism developed by Szegedy [31]. The latter formalism is able to describe QWs on directed and weighted networks by means of quantized Markov chains. Connections between coined and Szegedy QWs have been established through staggered QWs [32, 33]. For an overview of QWs and search algorithms, see Ref. [34] and for yet other formulations of QWs see Refs. [32, 35–39].

For certain optimization problems it can be advantageous to employ search algorithms with stochastic resetting, since optimization strategies without reset may end up in regions far away from the actual solutions [40, 41]. Motivated by the success of random-walk-based search strategies [42, 43], we study stochastic quantum walks¹ with resetting on networks. Note that stochastic resetting has been also studied in the context of CRWs on networks [45] and QWs [46]. We introduce a unifying framework that enables us to interpolate between classical and quantum random-walk regimes and to analyze the influence of classical processes that perturb QWs, contributing to a better understanding of the physical robustness of certain quantum algorithms.

The paper is organized as follows. In Sec. II we briefly review some key concepts from the study of complex networks that will be exploited in our further analysis. In Sec. III we provide precise definitions of the CRWs and the QWs we consider and understand these walks as cornerstones for a linear interpolation scheme that allows us to add “classicality” to QWs and vice versa “quantumness” to CRWs. Our general formulation of classical, quantum, and hybrid classical-quantum walks

* swald@pks.mpg.de; Both authors contributed equally to this work.

† lucasb@ethz.ch

¹ What we refer to as QW is sometimes called *continuous quantum walk* [44]. We shall introduce the precise meaning in the following sections.

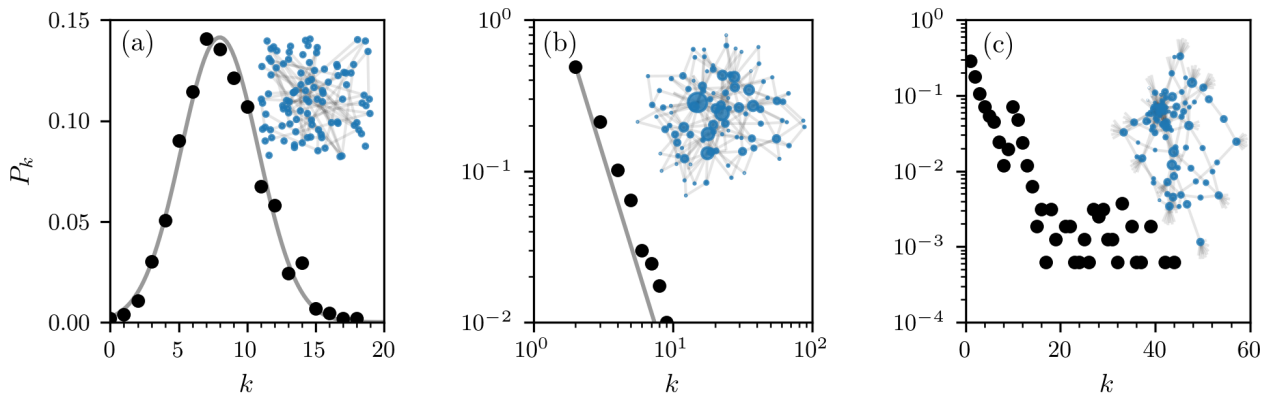


Figure 1. **Degree distributions of different networks.** We show the degree distributions of the different networks that we use throughout this work. Black disks represent the degree distribution of a particular network realization and the gray solid line is the corresponding analytic degree distribution. The insets show realizations of the networks. (a) Erdős-Rényi network with a Gaussian degree distribution and $N = 1600$ nodes. In the depicted realization, two nodes are connected with probability 5×10^{-3} . The network that we show in the inset has 100 nodes. (b) Barabási-Albert network with a power-law degree distribution. The corresponding exponent is -3 [20]. Each new node is connected to $m_0 = 2$ existing nodes and the depicted realization has $N = 1600$ nodes. The network that we show in the inset has 100 nodes and the sizes of its nodes scale with their betweenness centralities. (c) Peer-to-peer network (p2p-Gnutella08) [21] with $N = 1600$ nodes and mean degree $\bar{k} \approx 2.5$. The network that we show in the inset has 200 nodes and the sizes of its nodes scale with their betweenness centralities.

on networks utilizes the theoretical framework of quantum stochastic walks (QSWs) [47], which we tailor to account for stochastic resetting. We compare our analytical results with corresponding simulations on different networks in Secs. IV and V. In Sec. VI, we discuss our results and conclude.

II. NETWORK SCIENCE CONCEPTS

A graph G (i.e., a network) is an ordered pair of two sets $G = (V, E)$ where V is the set of *nodes* and $E \subseteq V \times V$ is the set of *edges*, respectively [48]. We denote the number of nodes by N (i.e., $|V| = N$). Throughout this paper, we consider undirected networks, meaning that all edges are bidirectional, with unweighted edges. In order to describe dynamics on such graphs, we introduce a Hilbert space structure in the standard way by assigning to each node i a basis vector $|i\rangle$. These basis vectors are chosen to be orthonormal, i.e. $\langle i | j \rangle = \delta_{ij}$. The *adjacency matrix* A of a graph G describes the connections of the graph. For undirected networks with unweighted edges, each matrix element $A_{ij} \in \{0, 1\}$ is

$$A_{ij} = \begin{cases} 1, & \text{if } (i, j) \in E, \\ 0, & \text{otherwise.} \end{cases} \quad (1)$$

The adjacency matrix is thus a symmetric binary matrix and can be written in Dirac notation as

$$A = \sum_{i, j \in V} A_{ij} |i\rangle \langle j|. \quad (2)$$

The *degree* k_i of node i is defined as the sum over the respective row of the adjacency matrix (i.e., $k_i =$

$\sum_{j=1}^N A_{ij}$) and counts the number of connections leading to (respectively away from) node i .

A characteristic quantity for graphs is the *degree distribution* that indicates the frequency of nodes with a certain degree. It is defined as $P_k = n_k/N$, where n_k is the number of nodes of degree k in G . The *degree matrix* D of G is

$$D = \sum_{i=1}^N k_i |i\rangle \langle i|. \quad (3)$$

D is a diagonal matrix whose elements correspond to the degree of the respective node. The evolution of CRWs and QWs on a graph $G(V, E)$ can be described by the *graph Laplacian* [49]

$$\mathbb{L} = D - A, \quad \mathbb{L}_{ij} = \begin{cases} k_i & \text{if } i = j \\ -1 & \text{if } (i, j) \in E \\ 0, & \text{otherwise} \end{cases}. \quad (4)$$

These theoretical tools suffice for the study of the types of random walks that we envision. We shall now specify the set of graphs that we use in the present work. While our analytic results can be applied to general graphs, we will focus on the following three different networks for explicit numerical verification of our results.

- **Erdős-Rényi:** Two nodes are connected with probability p , which is independent of all other connections. Erdős-Rényi graphs have a binomial degree distribution [48].
- **Barabási-Albert:** A new node will be attached to $m \leq m_0$ existing nodes and the attachment probability is proportional to the number of edges of the

existing nodes. This preferential-attachment process leads to a scale-free network with an algebraic degree distribution [20].

- **Peer-to-peer (p2p-Gnutella08)**: Nodes in this empirical network correspond to computers in a file-sharing network [21].

In Fig. 1 we show the degree distributions and exemplary realizations of these networks. Our choice of the outlined networks is motivated by their different connectivity patterns, which enable us to study how such differences affect the properties of CRWs and QWs.

III. QUANTUM STOCHASTIC WALKS ON NETWORKS

In this section, we shall specify the types of walks on graphs that we study in the present work. Our choice is not unique and we refer the reader to Refs. [34, 50] for an overview of different realizations of CRWs and QWs. The walks that we study in this work are schematically summarized in Fig. 2.

We start by introducing CRWs (Sec. III A) in terms of their probability distribution and QWs (Sec. III B) in terms of the corresponding wave function. CRWs and (continuous) QWs are fundamentally different as the latter are reversible as long as the walker is not measured, whereas the former are inherently irreversible. It has been argued that the characteristics of both types of dynamics can be incorporated in the dissipative dynamics of the density matrix of a quantum system, resulting in quantum stochastic walks (QSWs) [47]. General quantum stochastic processes can be described by a Lindblad master equation for the reduced density matrix ϱ of a quantum system² [51, 52]

$$\frac{d\varrho}{dt} = -i[H, \varrho] + \sum_n L_n \varrho L_n^\dagger - \frac{1}{2} \{L_n^\dagger L_n, \varrho\} = \mathcal{L}(\varrho). \quad (5)$$

Here, H is the quantum Hamiltonian of the system and L_n are certain quantum jump operators, each of which introduces a corresponding stochastic process to the dynamics of the quantum system. The generic solution of Eq. (5) with the initial density matrix $\varrho(0)$ can be written in terms of the time-independent superoperator \mathcal{L} as

$$\varrho(t) = e^{\mathcal{L}t} \varrho(0). \quad (6)$$

In the following sections, we employ a set of rules [47] to include CRWs as stochastic background to QWs and we shall see that each classically allowed transition will result in a dissipative contribution to the superoperator.

We proceed as follows. In Secs. III A and III B, we specify the types of CRWs and QWs on networks that

we study in this paper. These can be seen as cornerstones of the outlined theory. In Sec. III C, we introduce an interpolation scheme between these cornerstones and, in this way, define a quantum-to-classical random walk (QCW). Finally, in Sec. III D, we introduce stochastic resetting by means of a suitable quantum jump process.

A. Classical random walks on networks

We describe the evolution of a CRW on a network G in terms of the probabilities $p_i(t)$ of observing a walker on node i at time t . These probabilities form a normalized probability vector

$$\mathbf{p}(t) = (p_1(t), \dots, p_N(t)), \quad \sum_{i=1}^N p_i(t) = 1. \quad (7)$$

In the time interval $[t, t + \Delta t]$, conservation of probability implies that the local probabilities can only flow in and out of nodes. In particular, if Δt is small enough, the net-influx to node i originates from the immediate neighborhood of node i . The evolution of the probability $p_i(t)$ is thus described by the following rate equation

$$p_i(t + \Delta t) - p_i(t) = -\Delta t \left(p_i(t) - \sum_{j=1}^N \frac{A_{ij}}{k_j} p_j(t) \right). \quad (8)$$

The first term on the right-hand-side corresponds to the outward flow from node i to its surroundings and the second term describes the inflow to node i . We may rewrite Eq. (8) in matrix form

$$\frac{\mathbf{p}(t + \Delta t) - \mathbf{p}(t)}{\Delta t} = -\mathbb{L}D^{-1}\mathbf{p}(t), \quad (9)$$

with the graph Laplacian \mathbb{L} and the degree matrix D (see Eqs. (3) and (4)). In the limit $\Delta t \rightarrow 0$, this rate equation becomes a master equation in differential form

$$\frac{d}{dt}\mathbf{p}(t) = -H_c\mathbf{p}(t), \quad H_c = \mathbb{L}D^{-1}. \quad (10)$$

Here, we introduced the classical Hamiltonian H_c as generator of time translation of the probability distribution. Equation (10) is formally solved with the time evolution operator $S(t) = e^{-H_c t}$ which allows us to write the probability distribution at time t , that originated from an initial distribution \mathbf{p}_0 , as

$$\mathbf{p}(t) = S(t)\mathbf{p}_0. \quad (11)$$

For connected networks, meaning that for every pair of nodes (i, j) there exists a set of adjacent edges that connects i to j , and sufficiently long times, the CRW approaches a stationary probability distribution \mathbf{p}^* such that $p_i^* = \sum_{j=1}^N \frac{A_{ij}}{k_j} p_j^*$. This allows us to fully determine

² Here, $\hbar = 1$ and we apply this convention throughout the paper.

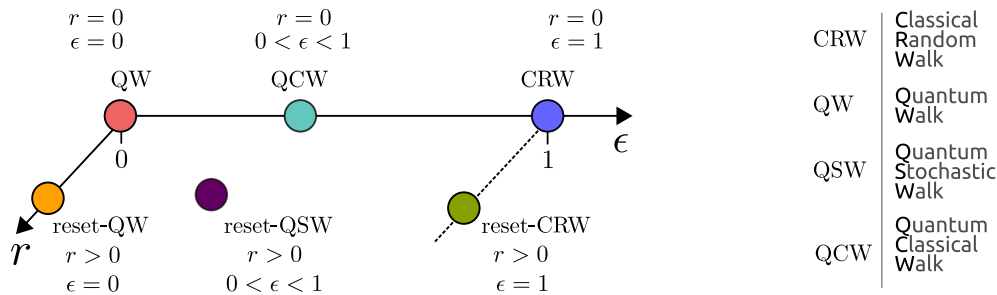


Figure 2. **Overview of different classical and quantum reset walks.** Different types of random walks as function of the classicality parameter ϵ (see Eq. (26)) and reset rate r (see Eq. (28)). The classicality parameter $0 \leq \epsilon \leq 1$ allows us to smoothly interpolate between a QW ($\epsilon = 0$) and a CRW ($\epsilon = 1$). In the time interval $[t, t + dt]$, a reset to the initial state occurs with probability $r dt$.

the stationary probability distribution as³

$$p_i^* = \frac{k_i}{\sum_{i=1}^N k_i}. \quad (12)$$

In the following sections, we will compare CRWs and QWs in terms of the probability p'_k that any node with degree k is occupied. The stationary probability p_i^* and the occupation probability p'_k are connected via the degree distribution P_k (see Sec. II) according to

$$p_i^* = p'_k P_k. \quad (13)$$

B. Quantum walks on networks

A quantum walker is described by its wave function $|\phi\rangle \in \mathbb{C}^N$ rather than a probability distribution. The wave function propagates according to the Schrödinger equation

$$\partial_t |\phi\rangle = -i H_q |\phi\rangle \quad (14)$$

with some quantum Hamiltonian H_q . This formulation of QWs is generally referred to as continuous time quantum walk [44]. We note that a QW, as defined in Eq. (14), is not inherently stochastic since the Schrödinger equation itself is deterministic. Stochasticity in QWs rather stems from measurements that are applied to the quantum system and lead to a collapse of the wave-function [36] as illustrated in Fig. 3. In analogy to a CRW (see Eq. (11)), the quantum Hamiltonian generates a quantum-time-evolution operator

$$U(t) = e^{-i H_q t} \quad (15)$$

for a QW on G . The choice of H_q thus determines the behavior of the QW. We follow Ref. [49] and choose the symmetric and normalized graph Laplacian

$$H_q = D^{-1/2} \mathbb{L} D^{-1/2} \quad (16)$$

as hermitian quantum Hamiltonian.⁴ QWs that are based on the Hamiltonian in Eq. (16) have the appealing property that the average probability to find the quantum walker on a certain node will be the same as in the classical case if the system is in the ground state (see Sec. III A) [49, 53].

In order to prepare the ground for more general QSWs, we replace the wave function $|\phi\rangle$ by the density matrix $\varrho = \sum_{ij} \varrho_{ij} |i\rangle \langle j|$ and the Schrödinger equation (see Eq. (14)) by the equivalent von-Neumann equation

$$\frac{d\varrho}{dt} = -i [H_q, \varrho]. \quad (17)$$

This formulation is able to account for statistical mixtures of wave functions and can be easily extended to open quantum systems as needed for classical-quantum mixtures of random walks. For the QW that results from Eqs. (16) and (17), the probability q_i^* of observing the walker at site i for large times is given by the long-time average

$$q_i^* = \frac{1}{T} \int_0^T \langle i | \varrho(t) | i \rangle dt. \quad (18)$$

Similar to the classical case, we denote by q'_k the probability that any node with degree k is populated. The probability q_i^* and q'_k are then again connected via

$$q_i^* = q'_k P_k. \quad (19)$$

C. Quantum-to-classical stochastic walks

Having outlined frameworks for the treatment of CRWs and QWs on networks, we now proceed and introduce a generalized QSW that interpolates between these walks. We recall that any QSW is described by the Lindblad

³ It is straightforward to check that \mathbf{p}^* is indeed the steady state by applying the classical Hamiltonian to Eq. (12).

⁴ Note that the classical Hamiltonian is not necessarily Hermitian since in general $[A, D^{-1}] \neq 0$ (for a lattice we though have $[A, D^{-1}] = 0$ since $D \propto \mathbb{1}$).

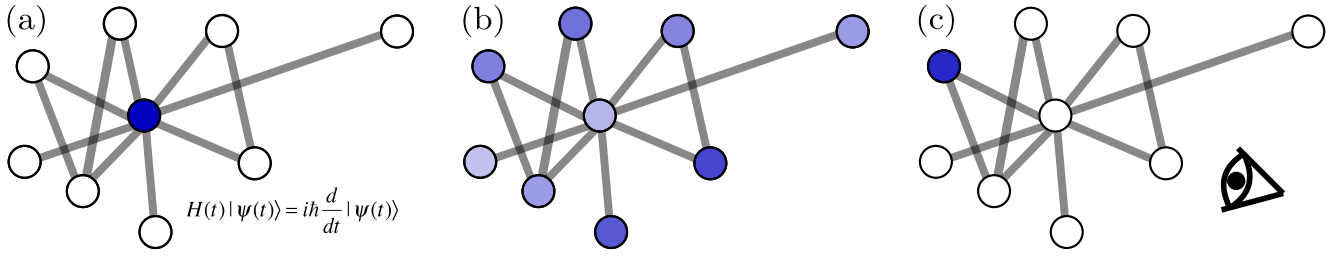


Figure 3. **Schematic of a quantum walk.** A quantum walker starts from a certain initial state in panel (a). Here the initial state is fully localized on a certain node for illustration purposes. The dynamics of the quantum walker is governed by the Schrödinger equation. After some time, the wave function of the walker will be spread over the network as depicted in panel (b) and there will be quantum superpositions. Knowing the initial state, both the Hamiltonian that induces the dynamics and the waiting time uniquely determine this state. Observing (or measuring) the quantum walker will result in a collapse of the wave function as shown in panel (c) and there is no way of knowing to which state the wave function collapses. This introduces stochasticity to QWs.

master equation (5) and introduce a dimensionless interpolation parameter ϵ in such a way that we recover the QW of Eq. (16) for $\epsilon = 0$. The choice

$$H = (1 - \epsilon)H_q, \quad L_n \propto \sqrt{\epsilon}, \quad \forall n \quad (20)$$

reduces the Lindblad master equation to the von-Neumann equation of the QW (see Eq. (17)), in the limit $\epsilon \rightarrow 0$.

In order to also account for CRW dynamics, we need to choose specific dissipative processes by specifying the quantum jump operators L_n . It has been shown that if the quantum jump operators satisfy the relation [47]

$$\sum_n \left(\delta_{ab} \langle a | L_n^\dagger L_n | a \rangle + \sum_m \langle a | L_n | b \rangle \langle b | L_m | a \rangle \right) = - \langle a | H_c | b \rangle, \quad (21)$$

the classical processes induced by the classical Hamiltonian are encompassed in the dynamics of the generalized quantum system. In order to proceed, we choose the set of quantum jump operators⁵

$$L_{nm} = \sqrt{\epsilon \gamma_{nm}} |n\rangle \langle m|, \quad (n, m) \in E. \quad (22)$$

L_{nm} induces jumps from node n to node m and satisfies

$$L_{nm}^\dagger L_{nm} = \epsilon \gamma_{nm} |m\rangle \langle m|. \quad (23)$$

The parameters $\gamma_{nm} \in \mathbb{R}$ are the so-called *damping constants*. We use Eqs. (21) and (22) to determine the damping constants and a rather straightforward calculation reveals

$$\gamma_{nm} = -\delta_{nm} + \frac{A_{nm}}{k_m} = - \langle n | H_c | m \rangle. \quad (24)$$

It is important to distinguish between diagonal and off-diagonal contributions. Based on Eq. (10), it is clear that the off-diagonal elements of the classical Hamiltonian are negative, rendering the damping constants γ_{nm} positive for $n \neq m$. For $n = m$, the entries of the classical Hamiltonian are equal to 1. Consequently, the parameter $\gamma_{nn} < 0$ and thus

$$L_{nn} = i\sqrt{\epsilon} |n\rangle \langle n|. \quad (25)$$

The full dynamics of a QCW is thus given by the Lindblad master equation

$$\frac{d\rho}{dt} = -i[(1 - \epsilon)H_q, \rho] + \epsilon \sum_{nm} \langle n | H_c | m \rangle \left[\varrho_{mm} |n\rangle \langle n| - \frac{1}{2} \{ |m\rangle \langle m|, \rho \} \right] \quad (26)$$

Based on this expression, it is possible to explicitly show that this QSW recovers the CRW (see Eq. (10)) in the limit $\epsilon \rightarrow 1$, see App. A for further details.

As the dissipator in Eq. (26) is well defined by the classical and quantum Hamiltonian and the parameter ϵ , we introduce the short-hand notation in terms of the superoperator

$$\frac{d\rho}{dt} = \mathcal{L}^{(\epsilon)}(\rho). \quad (27)$$

The QCW defined by Eq. (26) linearly interpolates between the CRWs and QWs that we defined in the preceding sections. This means that classical and quantum dynamics have been induced on the *same network* and that each link of this network is capable of hosting a classical and a quantum hopping process. One way to look at this is that finite thermal excitations in the system may introduce classical hopping on the quantum graph. This setup can be readily altered by, for instance, defining separate quantum and classical layers. We leave these directions for future works and focus instead on the dynamics induced by Eq. (26).

⁵ The explicit choice of the quantum jump operators is not unique.

D. Reset quantum stochastic walks on networks

We describe stochastic resets by an additional dissipative contribution in the evolution of QCWs (see Eq. (26)) [54]. The modified Lindblad master equation including a reset process with a certain rate r to the initial state $\varrho(0)$ reads [54, Eq. (59)]

$$\partial_t \varrho = \mathcal{L}^{(\epsilon)}(\varrho) + r\varrho(0) - r\varrho \equiv \mathcal{L}_r^{(\epsilon)}(\varrho). \quad (28)$$

In the case of a pure reset state, the reset density matrix may be written as a projector $\varrho(0) = |\phi(0)\rangle\langle\phi(0)|$. It turns out that the stationary state of the reset dynamics ϱ_r^* may be written explicitly in terms of left and right eigenmatrices and eigenvalues of the system without reset

$$\mathcal{L}_0^{(\epsilon)}(\mathbf{r}_n^{(\epsilon)}) = \lambda_n^{(\epsilon)} \mathbf{r}_n^{(\epsilon)}, \quad (\mathcal{L}_0^{(\epsilon)})^\dagger(\mathbf{l}_n^{(\epsilon)}) = \bar{\lambda}_n^{(\epsilon)} \mathbf{l}_n^{(\epsilon)}. \quad (29)$$

The stationary state then reads [54]

$$(\varrho_r^{(\epsilon)})^* = (\varrho_{r=0}^{(\epsilon)})^* + r \sum_{n=2}^{N^2} \frac{\langle\phi(0)|(\mathbf{l}_n^{(\epsilon)})^\dagger|\phi(0)\rangle}{\lambda_n^{(\epsilon)} - r} \mathbf{r}_n^{(\epsilon)}. \quad (30)$$

This holds for all $0 < \epsilon \leq 1$ and reset rates $r \geq 0$. In the case of a QW ($\epsilon = 0$), there is no stationary state without reset and Eq. (30) reduces to [54]

$$(\varrho_r^{(1)})^* = E\Lambda_r E^\dagger, \quad (31)$$

where E is the matrix of eigenvectors of the quantum Hamiltonian $H_q E = E\Lambda$ with $\Lambda_{ij} = \lambda_i \delta_{ij}$ and the elements of Λ_r are

$$(\Lambda_r)_{ij} = r \frac{\langle\phi(0)|e_j\rangle\langle e_i|\phi(0)\rangle}{r + i(\lambda_i - \lambda_j)}. \quad (32)$$

Equations (30) and (31) are remarkable since they express the stationary state of the reset dynamics in terms of the unperturbed system without reset (i.e., for $r = 0$). This means that, e.g. for a QW where $\epsilon = 0$, the stationary state for $r > 0$ is found analytically by diagonalizing the quantum Hamiltonian. Furthermore, for a general reset-QCW, the closed form allows us to determine the steady-state probability for the walker to be on node ℓ , viz.

$$(q_r^{(\epsilon)})_\ell^* = (q_0^{(\epsilon)})_\ell^* + r \sum_{n=2}^{N^2} \frac{\langle\phi(0)|\mathbf{l}_n^{(\epsilon)\dagger}|\phi(0)\rangle\langle\ell|\mathbf{r}_n^{(\epsilon)}|\ell\rangle}{\lambda_n^{(\epsilon)} - r}. \quad (33)$$

In the special case of a QW ($\epsilon = 0$), this formula reduces to [54]

$$(q_r^{(0)})_\ell^* = \sum_{j,k} \frac{r \langle\phi(0)|e_k\rangle\langle e_j|\phi(0)\rangle}{r + i(\lambda_k - \lambda_j)} \langle\ell|e_j\rangle\langle e_k|\ell\rangle, \quad (34)$$

where λ_k and $|e_k\rangle$ are the eigenvalues and the eigenvectors of the quantum Hamiltonian H_q

$$H_q |e_k\rangle = \lambda_k |e_k\rangle. \quad (35)$$

We note that for a CRW, respectively QCW with $\epsilon = 1$, it is also possible to directly determine the stationary probability distribution $\mathbf{p}^*(r)$. In an infinitesimal time interval $[t, t + dt]$, the classical walk starts from its initial state \mathbf{p}_0 with probability $r dt$. The corresponding reset times τ are exponentially distributed with probability-density function $\varphi(\tau) = r e^{-r\tau}$. If the reset rate is finite (i.e., $r > 0$), we find the corresponding stationary distribution (see App. B for further details)

$$\mathbf{p}^*(r) = \int_0^\infty \varphi(\tau) S(t) \mathbf{p}_0 d\tau = \frac{r}{\mathbb{1}(1+r) - AD^{-1}} \mathbf{p}_0. \quad (36)$$

IV. NUMERICAL RECIPES

In order to efficiently model classical and quantum random walks on large networks, we simulate the Lindblad master equation as *piecewise deterministic process*. The commonly used (but not unique) unfolding of the master equation (5) in terms of a stochastic Schrödinger equation reads [51, 52]

$$|d\phi\rangle = -iH_{\text{eff}}|\phi\rangle dt + \sum_n \left[\frac{L_n|\phi\rangle}{\sqrt{\langle\phi|L_n^\dagger L_n|\phi\rangle}} - |\phi\rangle \right] dN_n. \quad (37)$$

Here $|\phi\rangle$ is the wave function of a certain quantum trajectory and the Poisson increment dN_n describes a noisy contribution that is generated by the physical process belonging to the quantum jump operator L_n . In each simulation step, the system either performs a time evolution according to the effective (non-hermitian) Hamiltonian

$$H_{\text{eff}} = H - \frac{i}{2} \left[\sum_n L_n^\dagger L_n - \langle\phi|L_n^\dagger L_n|\phi\rangle \right] \quad (38)$$

or otherwise an instantaneous quantum jump dN_n occurs. Quantum jumps dN_n satisfy

$$dN_n dN_m = \delta_{nm} dN_n, \quad \langle dN_n \rangle = \langle\phi|L_n^\dagger L_n|\phi\rangle dt. \quad (39)$$

The probability that a jump process occurs in the time step dt is

$$P_j = \sum_n dt \langle\phi|L_n^\dagger L_n|\phi\rangle. \quad (40)$$

The average over independently sampled quantum trajectories (or respectively the long-time limit of a single trajectory) allows us to determine the results of the Lindblad master equation.

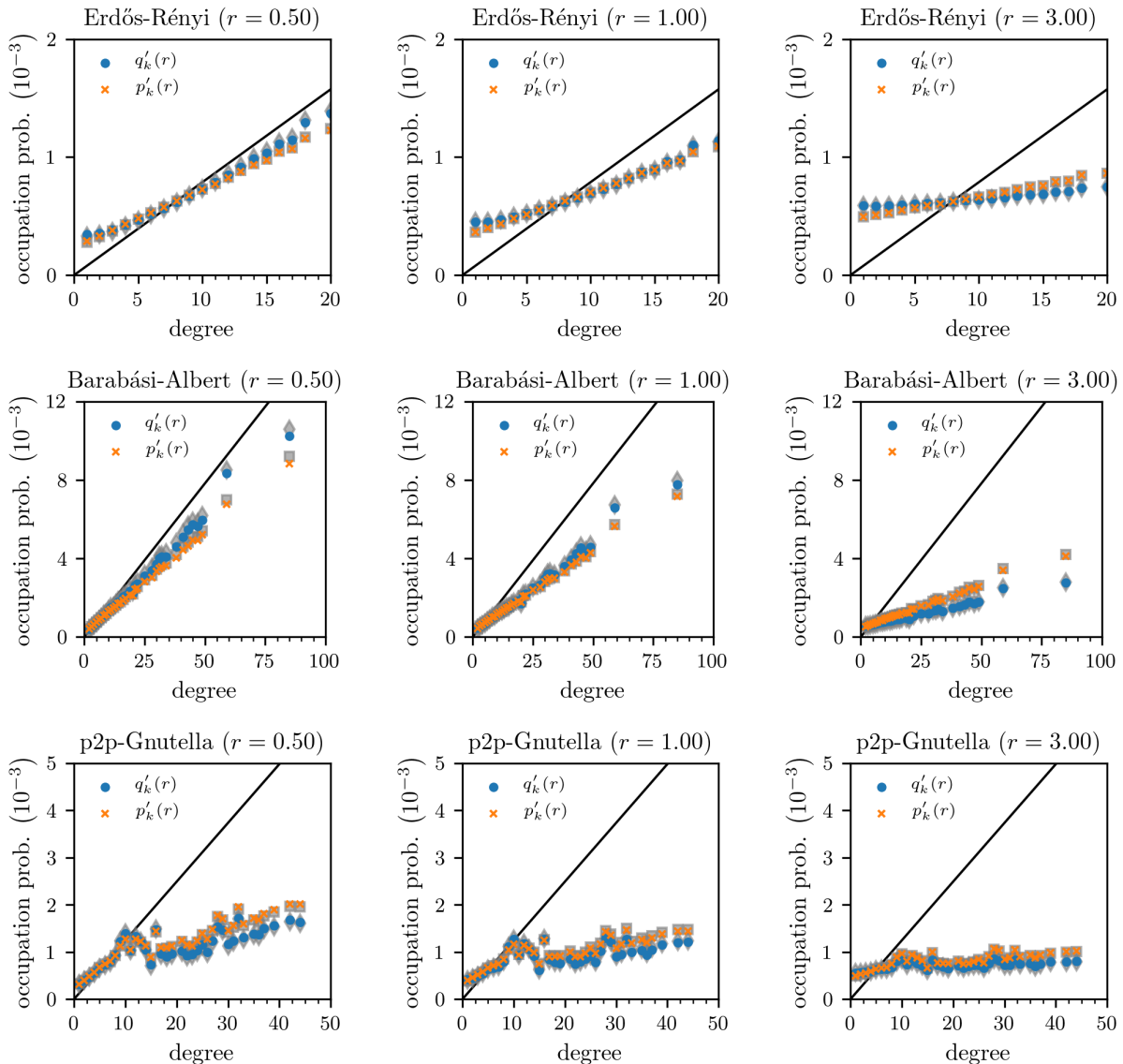


Figure 4. **Occupation probability for different networks and reset rates.** For different networks (row) and reset rates r (column), we show the probabilities $p'(r)$ and $q'(r)$ (see Eqs. (13) and (19)) that a node of degree k is occupied by a classical and quantum random walker, respectively. As initial conditions and reset states, we use states where every node is occupied with the same probability. Our numerical results are based on solutions of Eqs. (9) and (46). The networks we consider have $N = 1600$ nodes. The shown data points are averages over 2.5×10^5 samples. We use grey markers to indicate the solutions of the analytic results Eqs. (34) and (36). The black solid line is the occupation probability of a CRW for $r = 0$ as reference.

A. Stochastic Schrödinger equation for the reset dissipator

Here we discuss the numerical implementation of a quantum stochastic reset process for an otherwise unitary quantum walker. The inclusion of further dissipative processes is straightforward as the dissipative processes are additive in the Lindblad master equation (5). We shall exploit this fact in the next sections to write down the stochastic Schrödinger equation for a QCWs.

The quantum jump operators for the reset process pre-

sented in Sec. III D are [54]

$$J_n^r = \sqrt{r} |\phi(0)\rangle \langle n|. \quad (41)$$

From Eq. (37) we obtain the corresponding stochastic Schrödinger equation

$$|d\phi\rangle = r \sum_{n \in V} \left[\frac{\langle n | \phi \rangle}{|\langle \phi | n \rangle|} |\phi(0)\rangle - |\phi\rangle \right] dN_n - iH |\phi\rangle dt \quad (42)$$

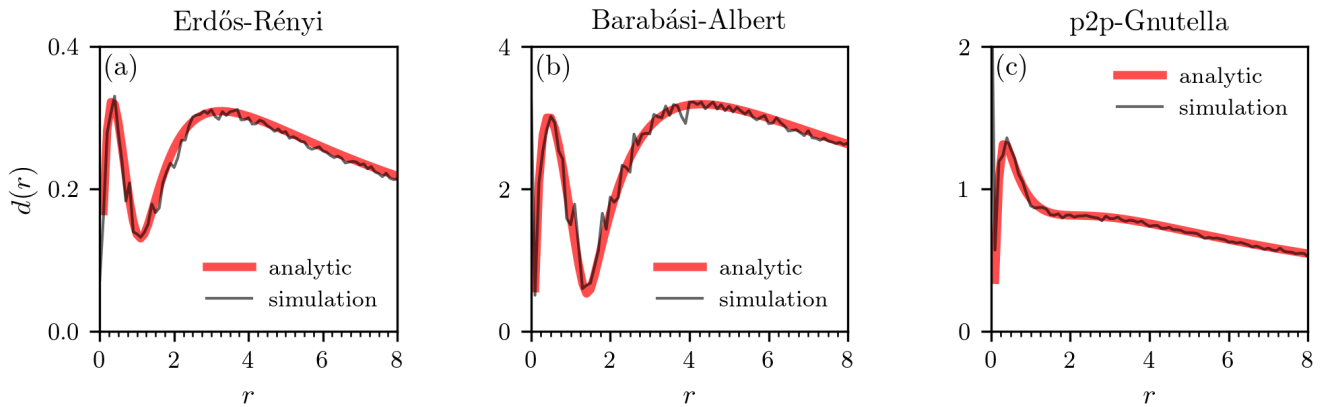


Figure 5. **Difference between the classical and quantum occupation probability for different networks and reset rates.** For different networks, we show the distance $d(r)$ (see Eq. (50)). As initial condition, we use stochastic vectors with uniformly distributed components between zero and one. Our numerical results are based on solutions of Eqs. (9) and (46). The networks we consider have $N = 1600$ nodes. The shown data points are averages over 2.5×10^5 samples.

with the quantum jump probability

$$P_j = r dt. \quad (43)$$

We see that the quantum jump probability corresponds to the reset rate and does not depend on the current quantum state, as it should be for a stochastic reset process. Furthermore, the only difference to a brute-force reset is a global phase that keeps information about the pre-reset state. Since this phase is global, we neglect it in the remainder and write

$$|d\phi\rangle = -iH|\phi\rangle dt + r \sum_{n \in V} \left[|\phi(0)\rangle - |\phi\rangle \right] dN_n. \quad (44)$$

This stochastic Schrödinger equation then yields the following simple stochastic rule for the time evolution of a unitary process with dissipative stochastic resets

$$|\phi(t+dt)\rangle = [1 - iH_q dt] |\phi(t)\rangle \Theta(z - r dt) + |\phi(0)\rangle \Theta(r dt - z) \quad (45)$$

with a uniformly distributed random number $z \in [0, 1]$ and the Heaviside step function $\Theta(x)$, which is 1 for $x \geq 0$ and 0 otherwise. This description of quantum reset processes has been also used in previous studies [46, 54].

In order to efficiently simulate the stochastic process induced by the reset (see Eq. (45)), we use a Crank-Nicholson scheme [55]:

$$|\phi^{n+1}\rangle = \begin{cases} |\phi(0)\rangle & \text{if } z \leq r dt, \\ |\phi^{n-1}\rangle - 2i\Delta t H_q |\phi^n\rangle & \text{otherwise,} \end{cases} \quad (46)$$

where the superscript n indicates the time step. For reset-CRWs, we use Eq. (45) and replace $|\phi\rangle$ by the probability vector \mathbf{p} and iH_q by the classical Hamiltonian H_c . To solve the evolution of CRWs, we use an Euler forward integration scheme.

B. Classical-to-quantum walks

In Sec. III, we introduced the quantum jump operators

$$L_{nm} = \sqrt{\epsilon} \sqrt{\langle n | H_c | m \rangle} |n\rangle \langle m| \quad (47)$$

to include the CRW in a quantum process. The resulting master equation of the QCW is Eq. (26) and the corresponding unravelling (see Eq. (37)) can be written as

$$|d\phi\rangle = -i(1 - \epsilon)H_q |\phi\rangle dt + \sum_{n, m \in V} \left[\frac{\langle m | \phi \rangle}{|\langle m | \phi \rangle|} e^{i\frac{\pi}{2}\delta_{nm}} |n\rangle - |\phi\rangle \right] dN_{nm} \quad (48)$$

with the Kronecker delta δ_{nm} . The quantum jump probability belonging to this stochastic Schrödinger equation reads

$$P_j = \epsilon dt \left(1 - \sum_{n \neq m \in V} \langle n | H_c | m \rangle |\langle m | \phi \rangle|^2 \right) = 2\epsilon dt \quad (49)$$

where the first equality is the definition of the jump probability for the previously defined set of quantum jump operators and the second equality is a direct consequence of the specific shape of the classical Hamiltonian and the symmetry of the adjacency matrix. Note that the dissipative processes in Eq. (48) do not contain the interpolation parameter ϵ . Rather the jump probability in Eq. (49) is proportional to ϵ , rendering quantum jumps impossible in the unitary limit $\epsilon \rightarrow 0$.

V. NUMERICAL RESULTS

A. Classical and quantum walks with resetting

We now compare our analytical results of the stationary states of reset QSWs (see Eq. (33) and (34)) with the corresponding numerical solutions, given an underlying reset

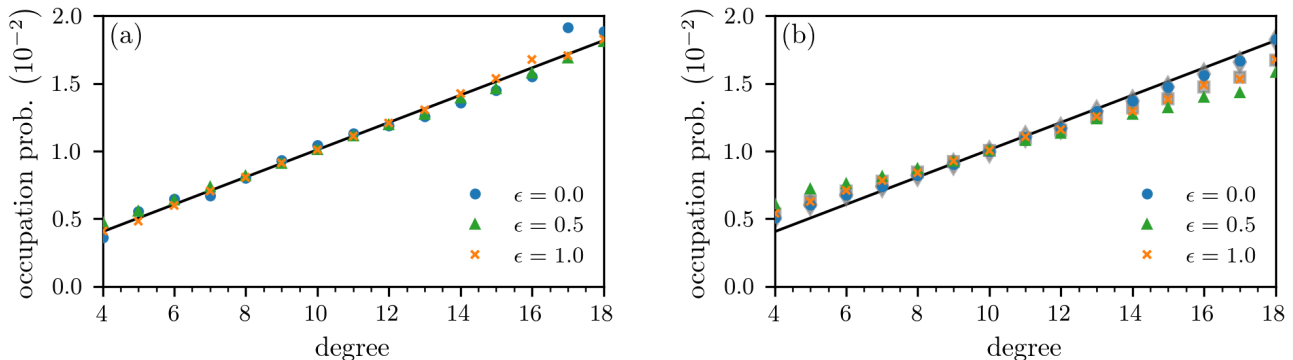


Figure 6. **Occupation probability for quantum-to-classical walks.** We show the probability that a node of degree k is occupied by a classical-to-quantum random walker for (a) $r = 0$ and (b) $r = 0.3$. As initial conditions and reset states, we use uniform states where every node is occupied with the same probability. Our numerical results are based on solutions of Eq. (48). Simulations were performed on an Erdős-Rényi network with $N = 100$ nodes. The shown data points are averages over 2×10^5 samples. The black solid line is the occupation probability of a CRW for $r = 0$ and grey markers in panel (b) correspond to analytical solutions for $\epsilon = 0, 1$.

process with rate r . In Fig. 4, we show the probabilities $p_k'(r)$ and $q_k'(r)$ that a node of degree k is occupied by a classical and quantum random walker, respectively (see Eqs. (13) and (19)). We perform simulations on Erdős-Rényi, Barabási-Albert, and peer-to-peer networks (see Sec. II). The degree distribution of Erdős-Rényi networks is binomial whereas Barabási-Albert networks and the peer-to-peer networks exhibit broader degree distributions (see Fig. 1). As initial condition and reset state, we use states where every node is occupied with the same probability. Thus, in the limit $r \rightarrow \infty$, the occupation probabilities satisfy $p_k'(r) = q_k'(r) = \text{const.}$ for all degrees k . Our results show that solutions of Eqs. (34) and (36) agree well with the numerically-obtained occupation probabilities $\mathbf{p}'(r)$ on all networks for different reset rates r .

We observe that the underlying network structure has a significant effect on how the occupation probabilities of the CRW and QW approach the limiting uniform distribution as r becomes larger. In the Supplemental Material [56], we include an animation of the occupation-probability evolution for the three aforementioned networks. Quantum walks sample from the occupation probability distribution in a different way than CRWs. For an Erdős-Rényi network and a reset rate $r = 0.5$, low and high degree nodes are more likely to be sampled by a QW than by a CRW, which is different from what we observe for Barabási-Albert and peer-to-peer networks (see Fig. 4). For a given network, this difference in sampling can be controlled with the reset rate r .

To determine the difference between $\mathbf{p}'(r)$ and $\mathbf{q}'(r)$ as a function of r , we define the distance metric

$$d(r) = \|\mathbf{p}'(r) - \mathbf{q}'(r)\|, \quad (50)$$

where $\|\cdot\|$ denotes the Euclidean norm. In Fig. 5, we show $d(r)$ for the three networks of Sec. II. Numerical and an-

alytical results are indicated by red and black solid lines, respectively. The distance between $\mathbf{p}'(r)$ and $\mathbf{q}'(r)$ is small, yet finite, for $r = 0$ and vanishes as $r \rightarrow \infty$. Interestingly, we observe multiple inflection points in $d(r)$ for the Erdős-Rényi and Barabási-Albert networks and a maximum distance $d(r)$ at $r \approx 0.3$ for the peer-to-peer and Erdős-Rényi networks. After the initial local minimum at $r \approx 0$, the distance between the classical and quantum occupation-probability distributions reaches a second pronounced local minimum at $r \approx 1$ and at $r \approx 1.5$ for the Erdős-Rényi and Barabási-Albert networks, respectively. Each minimum corresponds to a cross-over of $\mathbf{p}'(r)$ and $\mathbf{q}'(r)$. Based on the observed behavior of $\mathbf{p}'(r)$, $\mathbf{q}'(r)$, and $d(r)$, we conclude that classical and quantum occupation probabilities strongly depend on the underlying network structure and are not affected in the same way by changes of the reset rate r .

B. Reset quantum-to-classical walks

Figures 6 (a) and (b) show the occupation probability distribution of a QCW (see Eq. (48)) with $r = 0, 0.3$ and $\epsilon = 0, 0.5, 1$ on an Erdős-Rényi network. Note that the limits $\epsilon = 0$ and $\epsilon = 1$ correspond to the purely quantum and classical case, respectively. For $\epsilon = 0.5$, we obtain a hybrid quantum-to-classical walk with yet different node-occupation statistics. We observe that the occupation probability distribution of QCWs with $\epsilon = 0$ and $r = 0$ agrees with that of a CRW. We also find that a reset rate $r = 0.3$ leads to a qualitatively similar behavior between the QSW in its $\epsilon = 0, 1$ limits and the QWs and CRWs (see Fig. 3). Interestingly, the hybrid classical-quantum walk with $\epsilon = 0.5$ is affected more by the finite reset rate $r = 0.3$ than its purely classical and quantum counterparts.

VI. DISCUSSION AND OUTLOOK

Random walks are important models of diffusive processes in many branches of science. In this work, we introduced frameworks for the study of classical and quantum random walks with stochastic resetting on networks. We derived analytical solutions for the probability that a random walker occupies a certain node on a network. These analytical results, valid for general reset rates and network structures, are in perfect accordance with numerical solutions of the underlying master equations. Our results also revealed differences in the way classical and quantum walks with reset sample nodes with certain degrees. Both walks react differently to changes in the reset rate, which may be used as a control parameter to achieve desired node occupation (or sampling) statistics in quantum search and optimization algorithms [25, 57, 58]. For the networks that we studied in this paper, quantum walks approach the chosen reset distribution faster than classical walks. After formulating the classical and quantum dynamics of the random walker, we also proposed a quantum-to-classical walk, which interpolates between the classical and quantum limits, to study the effect of classical perturbations on QW dynamics.

Our study opens up several possible new directions of research on classical, quantum, and hybrid classical-quantum random-walk dynamics on networks. It has been suggested that Anderson-like localization can be observed in network dynamics upon changing the network topology rather than the disorder strength [59, 60]. In particular, the clustering of the underlying network induces a localization transition. The formalism that we outlined in this paper makes it possible to systematically investigate differences in quantum and classical Anderson-like transitions. Moreover, one could investigate how robust a localization transition is with respect to stochastic resetting that lifts localization at a fixed rate.

Another possible direction for future research is to extend our study to multilayer and temporal networks, thus accounting for more complex interaction structures and temporal features that may be relevant for the physical implementation of quantum walks [61]. In this context, it could be interesting to study transport properties in competing classical and quantum channels with distinct network structures. One particularly interesting case are several quantum graphs that are interconnected by classical links.

Furthermore, it is known that external constraints on single particle systems may introduce the notion of phase transitions on the mean-field level [62]. It would thus be interesting to study a random walker that is subject to a certain set of constraints and see how they affect transport and localization properties.

All codes and further detailed descriptions are publicly available on GitHub [63].

ACKNOWLEDGMENTS

We thank M Henkel, M Heyl and F Semião for helpful comments. LB acknowledges financial support from the SNF Early Postdoc.Mobility fellowship on “Multispecies interacting stochastic systems in biology” and from the Army Research Office (W911NF-18-1-0345).

Appendix A: Inclusion of CRW in QSW

In this appendix we show that the construction outlined in Sec. III C reduces to the CRW (see Eq. (10)) in the limit $\epsilon \rightarrow 1$. This is done by evaluating the time evolution of the corresponding occupation probabilities $p_\ell(t) = \langle \ell | \varrho | \ell \rangle$. We utilize the Lindblad master equation (26) to derive the time evolution of the probabilities, viz.

$$\frac{dp_\ell}{dt} = \sum_{n \neq m} \langle n | H_c | m \rangle \left[\frac{\varrho_{m\ell} + \varrho_{\ell m}}{2} \delta_{m\ell} - p_m \delta_{n\ell} \right] \quad (\text{A1})$$

It is then clear that we can reduce the double sum to a single sum due to the Kronecker delta terms and we see that there are two distinct contributions, viz.

$$\frac{dp_\ell}{dt} = \sum_{m \neq \ell} - \langle \ell | H_c | m \rangle p_m + \sum_{n \neq \ell} \langle n | H_c | \ell \rangle p_n \quad (\text{A2})$$

The first term is already in the correct shape to reproduce the classical dynamics and solely the diagonal contributions are differ. We need to use the explicit form of the classical Hamiltonian, in particular that the diagonal elements are equal to 1 in order to rewrite the second contribution. It is then straightforward to carry the calculation out as

$$\begin{aligned} \frac{dp_\ell}{dt} &= \sum_{m \neq \ell} - \langle \ell | H_c | m \rangle p_m - \sum_{n \neq \ell} \frac{A_{n\ell}}{k_\ell} p_n \\ &= \sum_{m \neq \ell} - \langle \ell | H_c | m \rangle p_m - p_\ell \\ &= \sum_m - \langle \ell | H_c | m \rangle p_m \end{aligned} \quad (\text{A3})$$

where we also used the symmetry of the adjacency matrix $A_{nm} = A_{mn}$. This proves that the generated dynamics coincides with the stochastic dynamics defined in Eq. (10).

Appendix B: Resolvent of infinitesimal generator

In this appendix, we illustrate the use of resolvents to formally solve differential equations. We consider the matrix differential equation

$$\dot{\mathbf{x}} = \mathbf{A} \mathbf{x}. \quad (\text{B1})$$

for the vector function $\mathbf{x} = (x_1, \dots, x_d)$ and $A \in \mathbb{R}^{d \times d}$. We introduce the Laplace transform $\hat{\mathbf{x}}(s)$ of $\mathbf{x}(t)$ as

$$\hat{\mathbf{x}}(s) = \int_0^\infty \mathbf{x}(t)e^{-st} dt. \quad (\text{B2})$$

Applying the Laplace transform to Eq. (B1) yields

$$\hat{\mathbf{x}}(s)s - \mathbf{x}(0) = A\hat{\mathbf{x}}(s). \quad (\text{B3})$$

In this way we reduced the differential equation (B1) to an algebraic equation

$$\hat{\mathbf{x}}(s) = (\mathbb{1}s - A)^{-1}\mathbf{x}(0), \quad (\text{B4})$$

whose solution is readily found. The operator $(\mathbb{1}s - A)^{-1}$ is called the *resolvent* of A [64]. An integral representa-

tion of the resolvent is found by applying the Laplace transform directly to the solution of Eq. (B1), we find

$$\mathbf{X}(s) = \int_0^\infty e^{-st}e^{At}\mathbf{x}(0) dt. \quad (\text{B5})$$

Combining Eqs. (B3) and (B5) yields

$$\int_0^\infty e^{-st}e^{At}\mathbf{x}(0) dt = (\mathbb{1}s - A)^{-1}\mathbf{x}(0). \quad (\text{B6})$$

This identity is used in Eq. (36) in order to explicitly determine the stationary state of the CRW.

-
- [1] K. Pearson, *Nature* **72**, 342 (1905).
[2] A. Einstein, *Annalen der Physik* **322**, 549 (1905).
[3] M. Kac, *The American Mathematical Monthly* **54**, 369 (1947).
[4] R. A. Epstein, *The theory of gambling and statistical logic* (Academic Press, 2012).
[5] P. J. Flory and M. Volkenstein, *Biopolymers: Original Research on Biomolecules* **8**, 699 (1969).
[6] M. Rubinstein, R. H. Colby, *et al.*, *Polymer physics*, Vol. 23 (Oxford university press New York, 2003).
[7] P. D. Gujrati and A. I. Leonov, *Modeling and simulation in polymers* (John Wiley & Sons, 2010).
[8] B. B. Mandelbrot, *Scientific American* **280**, 70 (1999).
[9] B. G. Malkiel, *A random walk down Wall Street: including a life-cycle guide to personal investing* (WW Norton & Company, 1999).
[10] A. Mårell, J. P. Ball, and A. Hofgaard, *Canadian Journal of Zoology* **80**, 854 (2002).
[11] F. Bartumeus, M. G. E. da Luz, G. M. Viswanathan, and J. Catalan, *Ecology* **86**, 3078 (2005).
[12] C. Gkantsidis, M. Mihail, and A. Saberi, in *IEEE INFOCOM 2004*, Vol. 1 (IEEE, 2004).
[13] L. Page, S. Brin, R. Motwani, and T. Winograd, *The pagerank citation ranking: Bringing order to the web.*, Tech. Rep. (Stanford InfoLab, 1999).
[14] M. H. DeGroot, *Journal of the American Statistical Association* **69**, 118 (1974).
[15] L. Böttcher, P. Montealegre, E. Goles, and H. Gersbach, *Physica A: Statistical Mechanics and its Applications* **545**, 123713 (2020).
[16] L. Böttcher and H. Gersbach, arXiv preprint arXiv:2001.05163 (2020).
[17] D. Ben-Avraham and S. Havlin, *Diffusion and reactions in fractals and disordered systems* (Cambridge university press, 2000).
[18] J. D. Noh and H. Rieger, *Physical Review Letters* **92**, 118701 (2004).
[19] N. Masuda, M. A. Porter, and R. Lambiotte, *Physics Reports* **716**, 1 (2017).
[20] R. Albert and A.-L. Barabási, *Reviews of modern physics* **74**, 47 (2002).
[21] J. Leskovec and A. Krevl, “SNAP Datasets: Stanford large network dataset collection,” <http://snap.stanford.edu/data> (2014).
[22] J. Watrous, *Journal of computer and system sciences* **62**, 376 (2001).
[23] P. Lecca and A. Re, *Theoretical Physics for Biological Systems* (CRC Press, 2019).
[24] N. Shenvi, J. Kempe, and K. B. Whaley, *Physical Review A* **67**, 052307 (2003).
[25] A. M. Childs and J. Goldstone, *Physical Review A* **70**, 022314 (2004).
[26] A. Tulsi, *Physical Review A* **78**, 012310 (2008).
[27] F. Magniez, A. Nayak, J. Roland, and M. Santha, *SIAM Journal on Computing* **40**, 142 (2011).
[28] A. M. Childs, *Physical Review Letters* **102**, 180501 (2009).
[29] Y. Aharonov, L. Davidovich, and N. Zagury, *Physical Review A* **48**, 1687 (1993).
[30] D. Aharonov, A. Ambainis, J. Kempe, and U. Vazirani, in *Proceedings of the thirty-third annual ACM symposium on Theory of computing* (2001) pp. 50–59.
[31] M. Szegedy, in *45th Annual IEEE symposium on foundations of computer science* (IEEE, 2004) pp. 32–41.
[32] R. Portugal, *Physical Review A* **93**, 062335 (2016).
[33] R. Portugal, R. A. Santos, T. D. Fernandes, and D. N. Gonçalves, *Quantum Information Processing* **15**, 85 (2016).
[34] R. Portugal, *Quantum walks and search algorithms* (Springer, 2013).
[35] G. Leung, P. Knott, J. Bailey, and V. Kendon, *New Journal of Physics* **12**, 123018 (2010).
[36] B. Kollár, T. Kiss, J. Novotný, and I. Jex, *Physical review letters* **108**, 230505 (2012).
[37] C. Chandrashekar and T. Busch, *Scientific reports* **4**, 6583 (2014).
[38] F. Elster, S. Barkhofen, T. Nitsche, J. Novotný, A. Gábris, I. Jex, and C. Silberhorn, *Scientific reports* **5**, 13495 (2015).
[39] A. Ghosal and P. Deb, *Physical Review A* **98**, 032104 (2018).
[40] M. Luby, A. Sinclair, and D. Zuckerman, *Information Processing Letters* **47**, 173 (1993).

- [41] M. Montero, A. Masó-Puigdellosas, and J. Villarroel, *The European Physical Journal B* **90**, 176 (2017).
- [42] B. Ham, D. Min, and K. Sohn, *IEEE transactions on image processing* **22**, 2574 (2013).
- [43] A. Valdeolivas, L. Tichit, C. Navarro, S. Perrin, G. Odelin, N. Levy, P. Cau, E. Remy, and A. Baudot, *Bioinformatics* **35**, 497 (2019).
- [44] S. E. Venegas-Andraca, *Quantum Information Processing* **11**, 1015 (2012).
- [45] A. P. Riascos, D. Boyer, P. Herringer, and J. L. Mateos, *Phys. Rev. E* **101**, 062147 (2020).
- [46] B. Mukherjee, K. Sengupta, and S. N. Majumdar, *Physical Review B* **98**, 104309 (2018).
- [47] J. D. Whitfield, C. A. Rodríguez-Rosario, and A. Aspuru-Guzik, *Physical Review A* **81**, 022323 (2010), [arXiv:0905.2942](https://arxiv.org/abs/0905.2942).
- [48] M. Newman, *Networks* (Oxford University Press, Oxford, 2018).
- [49] M. Faccin, T. Johnson, J. Biamonte, S. Kais, and P. Migdal, *Phys. Rev. X* **3**, 041007 (2013).
- [50] L. Böttcher and H. J. Herrmann, *Computational Statistical Physics (to appear)* (Cambridge University Press, Cambridge, 2020).
- [51] H. Breuer and F. Petruccione, *Theory of open quantum systems* (Oxford University Press, 2002).
- [52] G. Schaller, *Open Quantum Systems Far from Equilibrium*, Lecture Notes in Physics, Vol. 881 (Springer International Publishing, Cham, 2014).
- [53] J. Biamonte, M. Faccin, and M. De Domenico, *Communications Physics* **2**, 53 (2019), [arXiv:1702.08459](https://arxiv.org/abs/1702.08459).
- [54] D. C. Rose, H. Touchette, I. Lesanovsky, and J. P. Garrahan, *Physical Review E* **98**, 022129 (2018).
- [55] A. Askar and A. S. Cakmak, *The Journal of Chemical Physics* **68**, 2794 (1978).
- [56] S. Wald and L. Böttcher, “Evolution of occupation probabilities for different reset rates,” <https://vimeo.com/429312302> (2020).
- [57] B. L. Douglas and J. B. Wang, *J. Phys. A* **41**, 075303 (2008).
- [58] S. Chakraborty, L. Novo, A. Ambainis, and Y. Omar, *Physical review letters* **116**, 100501 (2016).
- [59] B. I. Shklovskii, B. Shapiro, B. R. Sears, P. Lambrianides, and H. B. Shore, *Phys. Rev. B* **47**, 11487 (1993).
- [60] L. Jahnke, J. W. Kantelhardt, R. Berkovits, and S. Havlin, *Phys. Rev. Lett.* **101**, 2 (2008).
- [61] J. Wang and K. Manouchehri, *Physical implementation of quantum walks* (Springer, Heidelberg, 2013).
- [62] S. Wald and M. Henkel, *Journal of Physics A: Mathematical and Theoretical* **49**, 125001 (2016).
- [63] “Github repository,” <https://github.com/lubo93/q2c-walks> (2020).
- [64] A. Pazy, *Semigroups of linear operators and applications to partial differential equations*, Vol. 44 (Springer Science & Business Media, 2012).